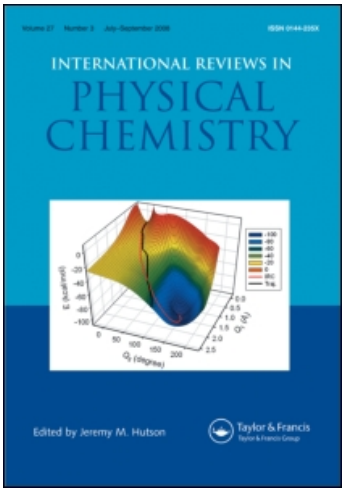

International Reviews in Physical Chemistry
Publication details, including instructions for authors and subscription information:
http://www.informaworld.com/smpp/title~content=t713724383

Atom-atom potentials from *ab initio* calculations

A. J. Stone[a]; A. J. Misquitta[a]
[a] University Chemical Laboratory, Cambridge CB2 1EW, UK

To cite this Article Stone, A. J. and Misquitta, A. J.(2007) 'Atom-atom potentials from *ab initio* calculations', International Reviews in Physical Chemistry, 26: 1, 193 — 222
To link to this Article: DOI: 10.1080/01442350601081931
URL: http://dx.doi.org/10.1080/01442350601081931

International Reviews in Physical Chemistry,
Vol. 26, No. 1, January–March 2007, 193–222

Taylor & Francis
Taylor & Francis Group

Atom–atom potentials from *ab initio* calculations

A. J. STONE* and A. J. MISQUITTA

University Chemical Laboratory, Lensfield Road, Cambridge CB2 1EW, UK

(*Received 12 September 2006; in final form 19 October 2006*)

Recent developments in *ab initio* intermolecular perturbation theory, using density functional theory, have made it possible to calculate intermolecular interactions between organic molecules of 30 or more atoms routinely and accurately. Related methods can provide accurate distributed properties of such molecules (multipoles and polarizabilities). These developments open up new possibilities for accurate *ab initio* atom–atom potentials, at a time when applications have raised new challenges, in that aspects of the interaction energy that were once ignored must now be accounted for. This review seeks to show how modern *ab initio* methods in intermolecular perturbation theory, and new methods for distributing molecular response properties, can be used to develop a new generation of atom–atom potentials.

Contents

*Corresponding author. Email: ajs1@cam.ac.uk

International Reviews in Physical Chemistry
ISSN 0144–235X print/ISSN 1366–591X online
http://www.tandf.co.uk/journals
DOI: 10.1080/01442350601081931

1. Introduction

For many purposes it is necessary to describe the interactions between molecules in a compact form that can be evaluated efficiently. Examples of such applications are simulations of molecules in the liquid or the solid, in solution or adsorbed on surfaces. In many such applications the molecules do not react, but retain their integrity and can often be treated as rigid or semi-rigid. Flexible molecules such as proteins raise additional issues, but there too there are interactions between different parts of the molecule that may come into close proximity to each other, and these interactions are similar to those between different molecules.

It is customary to describe these interactions in atom–atom form: that is, as a sum of terms, each describing the energy of interaction between a particular pair of atoms. In the past, such atom–atom terms have been derived by fitting a postulated functional form to experimental data, and there are a number of 'force fields', derived in this way, that are routinely used in simulations. However, it is becoming possible to derive accurate intermolecular potentials by *ab initio* calculation, and this offers a number of advantages. The main problem with empirical force fields is that the experimental data from which they are derived are determined by the interactions as a whole, and the individual terms that contribute to the interaction – dispersion, repulsion, electrostatic, induction – are not naturally separated. The force fields generally contain terms that correspond formally to these separate contributions, but the best fit to the data may not assign the contributions correctly. Any attempt to understand or interpret particular terms is then likely to be misleading.

Ab initio calculation, on the other hand, in the form of symmetry adapted perturbation theory (SAPT), leads to numerical values for each of the contributions, and these can then be described by analytical formulae in an appropriate way. The calculated values generally relate to the molecule as a whole, however, so it is still necessary to derive an atom–atom description in some way. We outline here the ways in which this can be done for each of the main terms in the interaction.

2. Defining an atom–atom potential

The starting point for our understanding of intermolecular forces is the many-body expansion, which is a partitioning of the N-body interaction energy. The leading terms describe two-body interactions, in which each pair of molecules in turn is treated as if no other molecules were present. The next terms describe three-body corrections – the correction that must be added to the sum of two-body terms to describe each set of three molecules correctly. This sequence continues through four-body and five-body corrections, and so on.

Formally, we define the interaction energy of a cluster of N interacting molecules as

$$\begin{aligned} V_{ABC\ldots}(\Omega_{ABC\ldots}) = E_{ABC\ldots}(\Omega_{ABC\ldots}, x_A^*, x_B^*, x_C^*, \ldots) \\ - E_A(x_A^0) - E_B(x_B^0) - E_C(x_C^0) - \cdots. \end{aligned} \tag{1}$$

Here $E_{ABC\ldots}$ is the energy of the cluster, E_X, $X = A, B, C$, etc., is the energy of molecule X; $\Omega_{ABC\ldots}$ describes the cluster geometry; x_X^0 is the geometry of monomer X in isolation; and x_X^* is the geometry that monomer X assumes in the cluster. We define $\delta E_X = E_X(x_X^*) - E_X(x_X^0)$, the change in internal energy of monomer X in going from geometry x_X^0 to geometry x_X^*, which will generally be positive. Then (1) can be re-written as

$$\begin{aligned} V_{ABC\ldots}(\Omega_{ABC\ldots}) &= E_{ABC\ldots}(\Omega_{ABC\ldots}, x_A^*, x_B^*, x_C^*, \ldots) - E_A(x_A^*) - E_B(x_B^*) - \cdots \\ &\quad + (E_A(x_A^*) - E_A(x_A^0)) + (E_B(x_B^*) - E_B(x_B^0)) + \cdots \\ &= V^*_{ABC\ldots}(\Omega_{ABC\ldots}) + \delta E_A + \delta E_B + \cdots, \end{aligned} \tag{2}$$

where $V^*_{ABC\ldots}$, implicitly defined above, can be regarded as the energy of the cluster relative to separated molecules held rigid in their cluster geometries.

We now expand $V^*_{ABC\ldots}$ in the many-body expansion:

$$V^*_{ABC\ldots} = \sum_{X<Y} V^*_{XY} + \sum_{X<Y<Z} \Delta V^*_{XYZ} + \cdots, \tag{3}$$

where ΔV^*_{XYZ} is the three-body correction, defined as

$$\Delta V^*_{XYZ} = V^*_{XYZ} - V^*_{XY} - V^*_{XZ} - V^*_{YZ}. \tag{4}$$

In the same way, we can define four-body corrections, five-body corrections, and so on.

The many-body expansion of the interaction energy is exact, but for it to be of practical use, the many-body corrections must be either small or easily obtained through a suitable approximation. The two-body interactions are well understood and can be evaluated for moderate-sized molecules, but accurate calculations of the many-body corrections are computationally very demanding and can be achieved for small clusters of small molecules only. Fortunately these corrections are usually relatively small, with the important exception of the three-body induction energy, which is often large but can be calculated to good accuracy if a good description of the molecular polarizability is available.

For practical reasons, therefore, we are led to concentrate on the pair interactions and the induction energy, both because they are the most important terms and because the other many-body terms are hard to calculate and are not well understood. We need an analytical representation of these terms for use in, say, simulations and geometry optimizations, applications that typically require the rapid evaluation of the interaction energy and perhaps its first and second derivatives. Current wisdom suggests that this surface is best constructed from a long-range, or asymptotic, part that is determined by the asymptotic forms of the interaction energy components and molecular properties, coupled with a short-range part that accounts for the exchange effects and other parts of the interaction energy not accounted for by the asymptotic expansion.

Perturbation theory provides an ideal framework for this paradigm, as it provides the interaction energy as a sum of physically understandable components, each of which has a well-defined analytical asymptotic form that depends only on the unperturbed properties of the interacting molecules. In fact, it is this separation and the resulting power of interpretation that has made perturbation theory the basis of most of the developments in the field of intermolecular interactions.

For the last ten years or so, the interaction energies were best calculated using the SAPT method of Jeziorski, Szalewicz *et al.* [1–3] which is based on Hartree–Fock theory. However this method uses a triple perturbation theory, the electron correlation in each monomer being treated as a perturbation along with the intermolecular interaction. Consequently the method, although accurate, is expensive in computer resources and cannot be applied to molecules of more than about 10 atoms. More recently, Szalewicz, Misquitta and Jeziorski [4, 5] have developed the SAPT(DFT) method, a perturbation theory based on density functional theory (DFT) and linear-response time-dependent density functional theory, while Hesselmann and Jansen [6–8] independently developed a very similar theory that they call DFT-SAPT. These methods retain the interpretative power and accuracy of SAPT while being much more efficient computationally, and they are well suited for accurate calculations on molecules of up to 20 or 30 atoms. SAPT(DFT) has been used to perform calculations on the RDX dimer (21 atoms per molecule) [9] and to generate the complete potential energy surface (PES) of the benzene dimer [10].

In brief, within the SAPT(DFT) formalism, the interaction energy components up to second order in the intermolecular perturbation operator are computed as follows. The first-order components, the electrostatic energy, $E^{(1)}_{\mathrm{elst}}$, and the first-order exchange energy, $E^{(1)}_{\mathrm{exch}}$, are computed using what is known as SAPT(KS), that is, a symmetry-adapted perturbation theory based on Kohn–Sham orbitals and eigenvalues [4, 6, 11, 12]. The SAPT(KS) expressions for the interaction energy components are identical to those from SAPT if the intramolecular correlation operators are neglected. Formally, given the exact functional, the ground-state electron density would be exactly recovered by Kohn–Sham density functional theory, so the electrostatic energy, which depends on the unperturbed charge densities of the interacting monomers (see below), should be recovered accurately within SAPT(KS). The first-order exchange energy depends on the ground-state wavefunctions of the monomers, so we might not expect this energy to be accurately recovered by SAPT(KS). However, $E^{(1)}_{\mathrm{exch}}$ depends on the wavefunctions through the interaction density matrix [13], and it has been shown [4, 12] that the asymptotic form of this quantity – which is most relevant for

intermolecular interactions – is the same for the Kohn–Sham wavefunctions as for the exact, implying that the SAPT(KS) expression for $E_{\text{exch}}^{(1)}$ should be very accurate. This has been borne out by numerous numerical tests on a variety of systems [4, 6, 12].

The second-order interaction energy components are response energies and cannot be described accurately within SAPT(KS), which takes no account of orbital response (relaxation) effects. Rather, these interaction energy components, which include the second-order induction energy, $E_{\text{ind}}^{(2)}$, and the second-order dispersion energy, $E_{\text{disp}}^{(2)}$, and their exchange counterparts (see section 6), are more correctly described using Kohn–Sham linear response theory (also known as coupled Kohn–Sham (CKS) theory), which describes the response of the orbitals to an external – possibly time-dependent – perturbation to first order in the perturbation. Both $E_{\text{ind}}^{(2)}$ and $E_{\text{disp}}^{(2)}$ can be expressed exactly in terms of the response functions from linear response theory, and these can be calculated exactly, in principle, within CKS theory. The second-order exchange energies have no simple expressions in terms of these response functions and so are calculated using scaling rules which have been demonstrated to work rather well [12, 14]. This formalism, that is, SAPT(KS) with CKS theory for the second-order components, is collectively termed SAPT(DFT). As yet, terms higher than second order in the interaction operator are not included in SAPT(DFT), but the third-order terms can be calculated using SAPT(KS), that is, without response effects. The higher-order terms can be important, and methods for approximating them will be discussed in section 7.

Being based on density functional theory, the accuracy achieved by SAPT(DFT) depends on the exchange-correlation functional used. Unlike supermolecular approaches to calculating the interaction energy, which vary quite strongly with functional, SAPT(DFT) interaction energies are quite robust and show only a weak dependence [12, 14]. However, the best results for large molecules have been obtained with the PBE0 hybrid functional [15] with the Tozer–Handy asymptotic correction [16, 17]. It is essential to apply an asymptotic correction, that is, to ensure the correct behaviour of the exchange–correlation potential at large distances, since that affects the long-range electron density, which in turn strongly influences the interaction energy components, particularly the first-order energies [4, 6]. Numerical details of the SAPT(DFT) method are fully described in [9, 14, 18].

It is now well understood that the asymptotic expansion must be of distributed form, that is, that we use a multi-centre rather than single-centre expansion. This is essential for large molecules, for which a single-centre expansion may not even converge, or if it does, the radius of divergence (the separation within which the expansion diverges) may be so large as to make the expansion meaningless. This then requires that molecular properties like the multipole moments, and the static and frequency-dependent polarizabilities on which the asymptotic expansions are based, be expressed in terms of multiple centres. The distribution of multipole moments was achieved over 25 years ago with the distributed multipole method (DMA) of Stone [19, 20] which has been recently refined [21] to accommodate the large basis sets used in modern accurate calculations. However the distribution of polarizabilities has proved a much harder problem, which has found a satisfactory solution [22–24] applicable to small organic molecules (containing perhaps as many as 30 atoms) only in the last few years.

Before the development of the SAFT(DFT) method, it was difficult, if not impossible, to compute accurate short-range interaction energies for all but the smallest of organic molecules. Consequently it was necessary to use the asymptotic forms of the interaction energy components, even at short-range, with the short-range exchange effects handled, if at all, by damping functions. This was a pragmatic approach but is undesirable and unnecessary today. The errors made by the asymptotic expansions can now be more fully understood and accounted for in the next generation of atom–atom potentials. There are indications of how this ought to be done and these will be described in section 9.

In the next few sections, we will consider the main components of the interaction energy in turn.

3. The electrostatic interaction

The electrostatic interaction arises from the straightforward classical interaction between the total ground-state charge densities of the interacting molecules:

$$E^{(1)}_{\mathrm{elst}} = \int \frac{\rho^A(\boldsymbol{r}_1)\rho^B(\boldsymbol{r}_2)}{|\boldsymbol{r}_1 - \boldsymbol{r}_2|}\, \mathrm{d}^3\boldsymbol{r}_1\, \mathrm{d}^3\boldsymbol{r}_2. \tag{5}$$

(Here and throughout we use atomic units.) In SAPT(DFT), the total charge densities that appear in this expression are evaluated using Kohn–Sham DFT.

Equation (5) can be broken down into atom–atom contributions in various ways. Formally all we have to do is to assign the charge density to regions surrounding each atom, to obtain

$$E^{(1)}_{\mathrm{elst}} = \sum_{a\in A}\sum_{b\in B} \int \frac{\rho^a(\boldsymbol{r}_1)\rho^b(\boldsymbol{r}_2)}{|\boldsymbol{r}_1 - \boldsymbol{r}_2|}\, \mathrm{d}^3\boldsymbol{r}_1\, \mathrm{d}^3\boldsymbol{r}_2 \tag{6}$$

where a denotes an atom of molecule A or the region associated with it, and $\sum_a \rho^a(\boldsymbol{r}) = \rho^A(\boldsymbol{r})$.

To obtain the asymptotic form of $E^{(1)}_{\mathrm{elst}}$, it is then necessary to represent the charge distribution $\rho^a(\boldsymbol{r})$ by a multipole expansion, using multipoles centred on the nucleus of atom a, at position $\boldsymbol{r}_a$:

$$Q^a_{lm} = \int \hat{Q}_{lm}(\boldsymbol{r} - \boldsymbol{r}_a)\rho^a(\boldsymbol{r})\, \mathrm{d}^3\boldsymbol{r}. \tag{7}$$

The assignment of charge density to atoms has been done in a number of ways [20, 25–29]. In Distributed Multipole Analysis (DMA) [19, 20], the electron density ρ_e is represented in terms of a Gaussian basis set:

$$\rho^A_e(\boldsymbol{r}) = \sum_{ij} D_{ij}\varphi_i(\boldsymbol{r})\varphi_j(\boldsymbol{r}) = \sum_{pq} C_{pq}\chi_p(\boldsymbol{r} - \boldsymbol{r}_p)\chi_q(\boldsymbol{r} - \boldsymbol{r}_q), \tag{8}$$

where the φ_i are contracted Gaussian basis functions and the $\chi_p(\boldsymbol{r}-\boldsymbol{r}_p)$ is a primitive Gaussian function centred at $\boldsymbol{r}_p$. The product $\chi_p(\boldsymbol{r}-\boldsymbol{r}_p)\chi_q(\boldsymbol{r}-\boldsymbol{r}_q)$ is another Gaussian centred at some point P_{pq} on the line between $\boldsymbol{r}_p$ and $\boldsymbol{r}_q$, and its contribution to the charge density can be represented by a short multipole expansion about P_{pq}. In the DMA method as originally proposed, this is in turn represented by a multipole expansion about the nearest site (which need not be at either $\boldsymbol{r}_p$ or $\boldsymbol{r}_q$).

This original DMA method is very sensitive to basis set, especially with the large basis sets containing diffuse functions that are now in common use. The problem may be illustrated by the case of CO_2. A diffuse p_z function on the C atom may be very similar to the difference $s_1 - s_2$ between diffuse s functions on oxygen atoms 1 and 2. Depending on the basis set in use, one or other description may be variationally preferred. However the density in the carbon p_z function is represented in the DMA method by a charge and quadrupole at the C atom, while the density in $s_1 - s_2$ is represented by charges on each oxygen atom. The resulting distributed multipole descriptions look very different. The electrostatic potential around the molecule is the same, to high accuracy, but there is no obvious convergence of the multipole description as the basis set is improved.

This problem has been overcome recently by a variation of the method [21], in which the part of the electron density arising from diffuse functions is integrated explicitly over the region around each atom. The resulting description converges steadily as the basis set is improved.

The main alternative approach to distributed multipole analysis is the method advocated by Popelier [29], in which the molecule is partitioned into atomic basins using Bader's method of atoms in molecules [30]. The integral of equation (7) is then taken over each atom basin in turn. This method is simple in concept, and the partition into atomic basins is well-defined and soundly based on theoretical principles, but the atom basins are sometimes awkwardly shaped, with the consequence that the resulting multipole expansions do not usually converge quite as well as the DMA, though Popelier has explored methods for improving the convergence [29]. A further disadvantage is that the partitioning procedure, and the ensuing integration, are relatively time-consuming.

There is a major limitation to any of these approaches: the electrostatic potential yielded by the multipole expansion is incorrect at any point within the charge distribution. The error, known as the penetration error, is particularly serious in hydrogen bonding, where the proton of the hydrogen bond often penetrates into the electron cloud of the acceptor atom [31]. In such cases the penetration error may be many $\mathrm{kJ\,mol^{-1}}$. We return to this issue in section 9.

4. First-order exchange–repulsion

The first-order exchange–repulsion energy, $E^{(1)}_{\mathrm{exch}}$, can be calculated very accurately using the SAPT(DFT) expressions [4, 12] at specified configurations of the interacting molecules. To obtain an atom–atom description of the exchange–repulsion entails breaking the molecule–molecule repulsion down into atom–atom terms. In this case there is no obvious analytical way of partitioning $E^{(1)}_{\mathrm{exch}}$, and numerical techniques or

approximations must be used. The simplest approach conceptually is to fit a suitable atom–atom potential function to a large dataset of interaction energies, calculated at a wide variety of distances and orientations of the interacting molecules. However, any fitting procedure that involves a large number of fitted parameters is liable to lead to non-physical values of some of the parameters. The simplest accurate description of atomic repulsions is the Born–Mayer form, which we write as

$$\sum_{a\in A}\sum_{b\in B} G\exp\bigl[-\alpha_{ab}(\Omega_{ab})\bigl(R_{ab}-\rho_{ab}(\Omega_{ab})\bigr)\bigr]. \tag{9}$$

Here $\rho_{ab}(\Omega_{ab})$ describes the shape of the interaction between atoms a and b as a function of their relative orientation Ω_{ab}, while α_{ab} similarly describes the hardness of the interaction. Often α_{ab} can be treated as constant, while $\rho_{ab}(\Omega_{ab})$ can usually be described by a short spherical-harmonic expansion. G is a constant energy unit; it can be seen that the repulsion between atoms a and b is equal to G when $R_{ab}=\rho_{ab}(\Omega_{ab})$, so that $\rho_{ab}(\Omega_{ab})$ describes the shape of the molecules at contour level G.

It is well established that for accurate treatments it is not sufficient to treat ρ as independent of orientation; indeed in some cases, notably halogens, the assumption of spherical atoms leads to results that are qualitatively wrong [32, 33].

Unfortunately, equation (9) then contains a large number of strongly-coupled parameters, even for molecules of quite modest size, and the fitting procedure has a strong tendency to lead to unphysical values for the parameters. It is necessary to find some way of separating the exchange–repulsion energy into atom–atom terms before attempting to fit it to an analytical expression. Fortunately this can be done. The method uses the density overlap model, which postulates that the exchange–repulsion energy is nearly proportional to the overlap between the molecular electron densities:

$$E^{(1)}_{\rm exch}=KS^{\gamma}_{\rho}, \qquad \text{where} \qquad \mathrm{S}_{\rho}=\int \rho_e^A(\boldsymbol{r})\rho_e^B(\boldsymbol{r})\,\mathrm{d}^3\boldsymbol{r}. \tag{10}$$

The exponent γ in this expression is close to 1 – typically in the range 0.96 to 0.99 – and for the exact density it is believed to be equal to 1 [34].

If indeed $\gamma=1$, we can partition the electron density into atomic contributions, so that $\rho^A(\boldsymbol{r}_e)=\sum_{a\in A}\rho^a(\boldsymbol{r}_e)$, and the exchange–repulsion energy then separates into atom–atom terms:

$$E^{(1)}_{\rm exch}=\sum_{a\in A}\sum_{b\in B}E^{(1)}_{\rm exch}[ab], \tag{11}$$

where

$$E^{(1)}_{\rm exch}[ab]=KS^{ab}_{\rho}=K\int \rho_e^a(\boldsymbol{r})\rho_e^b(\boldsymbol{r})\,\mathrm{d}^3\boldsymbol{r}. \tag{12}$$

Nobeli and Price [35] explored this approach, partitioning the density via a density-fitting procedure, and found that it was reasonably successful, though there

were difficulties with diffuse basis sets, and there is scope for refining the partitioning procedure, perhaps in a similar manner to that used for distributed multipoles. More generally, we may expect the proportionality constant to vary somewhat for different atom pairs:

$$E^{(1)}_{\mathrm{exch}}[ab] = K^{ab} S^{ab}_{\rho}, \tag{13}$$

where the constants K^{ab} could be determined by fits to $E^{(1)}_{\mathrm{exch}}$ calculated using SAPT(DFT) (but see also the discussion in section 9). Each of these atom–atom terms can then be fitted to a single Born–Mayer term or other analytical expression to obtain an analytical expression of the form equation (9), this time with physically sensible values for the parameters.

5. Induction and dispersion

The induction and dispersion interactions, although physically quite distinct, are both response energies, and share a common dependence on the frequency-dependent density susceptibility (FDDS) $\alpha(\boldsymbol{r}, \boldsymbol{r}'; \omega)$, which describes the change in electron density at $\boldsymbol{r}$ resulting from a delta-function perturbation in electrostatic potential at $\boldsymbol{r}'$, oscillating at frequency ω [36]. The induction energy of molecule A in an external potential $V(\boldsymbol{r})$ depends on the static FDDS:

$$E^{(2)}_{\mathrm{ind}}(A) = -\frac{1}{2}\int V(\boldsymbol{r}) V(\boldsymbol{r}') \alpha^{A}(\boldsymbol{r}, \boldsymbol{r}'; 0)\, \mathrm{d}^3\boldsymbol{r}\, \mathrm{d}^3\boldsymbol{r}', \tag{14}$$

while the dispersion energy between molecules A and B involves the FDDS of each molecule at imaginary frequency [36]:

$$E^{(2)}_{\mathrm{disp}} = -\frac{1}{2\pi}\int_0^{\infty} \mathrm{d}u \int \mathrm{d}^3\boldsymbol{r}_1\, \mathrm{d}^3\boldsymbol{r}'_1\, \mathrm{d}^3\boldsymbol{r}_2\, \mathrm{d}^3\boldsymbol{r}'_2 \frac{\alpha_A(\boldsymbol{r}_1, \boldsymbol{r}'_1; \mathrm{i}u)\alpha_B(\boldsymbol{r}_2, \boldsymbol{r}'_2; \mathrm{i}u)}{|\boldsymbol{r}_1 - \boldsymbol{r}_2||\boldsymbol{r}'_1 - \boldsymbol{r}'_2|}. \tag{15}$$

The FDDS calculated using Kohn–Sham linear response theory [37–39] has been used for some time now to obtain excitation energies of small systems [40] and recently it has been shown that this FDDS can also be used in accurate calculations of the dispersion and induction energies using (14) and (15). In fact, this is the basis of SAPT(DFT) and DFT–SAPT [5, 8]. Equations (14) and (15) are not evaluated directly in SAPT(DFT), but density-fitting techniques [41, 42] are used to recast these equations into a form that is more efficient computationally [9, 18, 43].

5.1. *Distributing the polarizabilities*

The asymptotic forms of expressions (14) and (15) depend on molecular multipole moments and static and frequency-dependent polarizabilities [44]. To obtain distributed form of these expressions we need distributed multipole moments and polarizabilities. The former have already been discussed above. It is not easy to find distribution

schemes for the polarizabilities that preserve accuracy, that make physical sense, and that are computationally cheap enough to be applicable to large molecules. Methods based on a real-space partitioning of the volumes surrounding each site, using either integration grids [45] or Bader's theory of atoms in molecules [46], result in non-local polarizabilities with large charge-flow terms which are hard to localize. Moreover, these methods lead to regions of fairly complex shape, which could lead to artifacts in the higher rank polarizabilities.

There are partitioning schemes based on fitting local polarizability models to the point-to-point polarizabilities computed on a grid around the molecule [22, 47]. In the Williams and Stone [22] implementation, compact and accurate local polarizability models can be constructed using this method, but polarizabilities of atomic sites buried under surface atoms are often unphysical. Furthermore, damping must be included in an empirical manner.

Other distribution methods have relied on basis-space partitioning schemes in which basis functions centred on a site are used to define the distributed polarizabilities involving that site. Early attempts based on this technique resulted in distributed polarizabilities that were not only very dependent on the basis set used but also completely unphysical in magnitude for larger, more complete, basis sets [48]. However, more recent attempts have been more successful. The LoProp method [49] uses a series of transformations to arrive at a localized orthonormal basis set that is then used to obtain distributed polarizabilities using the method of finite fields. LoProp is applicable to relatively large molecules and can use a variety of theory levels and basis sets, which is a considerable advantage. However, the finite-field method cannot be used to obtain frequency-dependent polarizabilities, and the calculation of high rank polarizabilities is difficult, so the the applicability of LoProp is limited.

More recently, Misquitta and Stone have developed a distribution scheme based on constrained density-fitting [23] that is applicable to large systems, without any of the limitations described above. However, rank for rank, the fitting technique of Williams and Stone results in more accurate polarizability models. As will be described below, the combination of these two methods yields a technique that is applicable to large molecules, results in physically acceptable local polarizabilities, and is very accurate, even when restricted to low rank.

In the Misquitta–Stone distribution scheme, one uses a modified density-fitting method [23]. The result of a coupled Kohn–Sham calculation of the FDDS is the set of coefficients in the molecular orbital expansion:

$$\alpha(\boldsymbol{r},\boldsymbol{r}';\omega)=\sum_{iv i'v'} C_{iv i'v'}(\omega)\varphi_i(\boldsymbol{r})\varphi_v(\boldsymbol{r})\varphi_{i'}(\boldsymbol{r}')\varphi_{v'}(\boldsymbol{r}'), \tag{16}$$

where the φ_i and φ_v are occupied and virtual molecular orbitals respectively. This expression can be simplified by expanding the transition densities $\varphi_i(\boldsymbol{r})\varphi_v(\boldsymbol{r})$ in terms of an auxiliary basis set $\{\chi\}$, so that the FDDS becomes

$$\alpha(\boldsymbol{r},\boldsymbol{r}';\omega)=\sum_{pq}\tilde{C}_{pq}(\omega)\chi_p(\boldsymbol{r})\chi_q(\boldsymbol{r}'). \tag{17}$$

Conventional molecular polarizabilities are readily obtained from the FDDS by an integration involving multipole moment operators. For example, the dipole–dipole polarizability involves the electric dipole moment operator:

$$\alpha_{\alpha\beta} = \int \hat{\mu}_\alpha(\boldsymbol{r})\hat{\mu}_\beta(\boldsymbol{r}')\alpha(\boldsymbol{r},\boldsymbol{r}';0)\,\mathrm{d}^3\boldsymbol{r}\,\mathrm{d}^3\boldsymbol{r}'. \tag{18}$$

Higher-rank polarizabilities (dipole–quadrupole, quadrupole–quadrupole, etc.) can be obtained by using the appropriate operators. In general, the polarizability $\alpha_{tu}(\omega)$ describes the response of the multipole moment Q_t to a field V_u oscillating at frequency ω:

$$\Delta Q_t(t) = -\alpha_{tu}(\omega)V_u \cos\omega t, \tag{19}$$

where

$$\alpha_{tu} = \int \hat{Q}_t(\boldsymbol{r})\hat{Q}_u(\boldsymbol{r}')\alpha(\boldsymbol{r},\boldsymbol{r}';\omega)\,\mathrm{d}^3\boldsymbol{r}\,\mathrm{d}^3\boldsymbol{r}'. \tag{20}$$

We use the generic suffices t and u to denote multipole moments and electric fields in a general way. They may take the values 00, 10, 11c, 11s, 20, ..., to describe the charge, the three dipole moment components, the five quadrupole moment components, and so on. In the case of the fields, V_{00} is the electrostatic potential, V_{10}, V_{11c} and V_{11s} are the three first derivatives (i.e., the components of the electric field, with a change of sign), and V_{20} etc. are the five spherical-tensor components of the second derivatives (field gradient). For more details of this notation, see [44].

Equations (18) and (20) describe molecular polarizabilities. Note that the multipole moment operators are implicitly defined with respect to some molecular origin. The ordinary dipole–dipole polarizability does not depend on the choice of origin, but the higher-rank polarizabilities do. Note also that there are no polarizabilities involving the total charge, since the charge on an isolated molecule cannot change.

We can obtain atom–atom polarizabilities in a similar manner by restricting the integration over $\boldsymbol{r}$ to some region a of the molecule, and the integration over $\boldsymbol{r}'$ to a region a'. The resulting polarizability describes the response at a' to a perturbation at a or *vice versa*:

$$\alpha_{tu}^{aa'} = \int_a \mathrm{d}^3\boldsymbol{r} \int_{a'} \mathrm{d}^3\boldsymbol{r}'\, \hat{Q}_t(\boldsymbol{r}-\boldsymbol{r}_a)\hat{Q}_u(\boldsymbol{r}'-\boldsymbol{r}_{a'})\alpha(\boldsymbol{r},\boldsymbol{r}';0). \tag{21}$$

The operators in this expression are referred to local origins at each atom, usually the nuclei. In this description, an external field $V_t(\boldsymbol{r}_a)$ at a induces changes in the moments Q_u^a at a, through the local polarizabilities α_{tu}^{aa}, and these in turn lead to induced moments at other atoms, which are described by the non-local polarizabilities $\alpha^{aa'}$ [44]. The external field $V_t(\boldsymbol{r}_a)$ therefore induces moments $V_t(\boldsymbol{r}_a)\alpha_{tu}^{aa'}$ at all the atoms of the

molecule. The total change $\Delta Q_u^{a'}$ involves a sum over all components of the fields at all atoms:

$$\Delta Q_u^{a'} = \sum_a \sum_t V_t(\boldsymbol{r}_a)\alpha_{tu}^{aa'}. \tag{22}$$

It is possible for the charge in any region of the molecule to change in response to a perturbation, so the description now includes charge-flow polarizabilities. The total charge still cannot change, and the atom–atom polarizabilities must satisfy sum rules to ensure that this is so [44, 50]. The induction energy of molecule A now takes the form

$$E_{\mathrm{ind}}(A) = -\frac{1}{2}\sum_{aa'}\sum_{tu} \alpha_{tu}^{aa'} V_t(\boldsymbol{r}_a) V_u(\boldsymbol{r}_{a'}), \tag{23}$$

where the sum is taken over sites in molecule A.

In the density-fitted representation, a natural way to restrict the integration to atom a is to include only the auxiliary basis functions on atom a:

$$\alpha_{tu}^{aa'} = \sum_{p\in a}\sum_{q\in a'} \tilde{C}_{pq} \int \mathrm{d}^3\boldsymbol{r}\, \hat{Q}_t(\boldsymbol{r}-\boldsymbol{r}_a)\chi_p(\boldsymbol{r}) \int \mathrm{d}^3\boldsymbol{r}'\, \hat{Q}_u(\boldsymbol{r}'-\boldsymbol{r}_{a'})\chi_q(\boldsymbol{r}'). \tag{24}$$

However this simple recipe leads to very unsatisfactory results. When the density-fitting basis $\{\chi\}$ contains diffuse functions, the diffuse functions on one atom may be used to describe features on another. The problem can be illustrated by the case of H_2 (table 1, taken from [23]). Equation (24) leads to the distributed polarizabilities shown in the column headed $\eta = 0.0$. These suggest that a unit potential difference between the atoms would lead to a flow of $131.56e$ from one atom to the other. This is clearly absurd, and although the large charge-flow is balanced by large dipole–charge and dipole–dipole polarizabilities in such a way as to lead to overall polarizabilities that are almost correct, the description is of no practical use.

We have overcome this problem by modifying the density-fitting algorithm. In the standard density-fitting procedure [41], the fitted density $\tilde{\rho}$ is found by minimizing the integrals

$$\Delta_{iv} = \int\int \big(\tilde{\rho}_{iv}(\boldsymbol{r}) - \rho_{iv}(\boldsymbol{r})\big)\frac{1}{|\boldsymbol{r}-\boldsymbol{r}'|}\big(\tilde{\rho}_{iv}(\boldsymbol{r}') - \rho_{iv}(\boldsymbol{r}')\big)\mathrm{d}^3\boldsymbol{r}\mathrm{d}^3\boldsymbol{r}', \tag{25}$$

where $\rho_{iv} = \varphi_i\varphi_v$ is one of the products of occupied and virtual Kohn–Sham orbitals that appear in equation (16). Formally, an orthogonality constraint should be applied:

$$d_{iv} = \int \tilde{\rho}_{iv}(\boldsymbol{r})\mathrm{d}^3\boldsymbol{r} = 0, \tag{26}$$

and although this is usually considered to be unnecessary, we have found that it improves the stability of the fitting procedure. More importantly, we have added a

Table 1. Total, distributed, and localized dipole–dipole polarizability components for the H_2 molecule. The hydrogen atoms are placed on the z-axis. All polarizabilities are in atomic units: $4\pi\epsilon_0 a_0^3$ for dipole–dipole, $4\pi\epsilon_0 a_0^2$ for dipole–charge, $4\pi\epsilon_0 a_0$ for charge–charge.

			Types of FDDS		
				DF: $\lambda = 1000.0$	
Sites	t	u	no-DF	$\eta = 0.0$	$\eta = 0.0005$
Total polarizabilities:					
	10	10	6.82	6.82	6.82
	11c	11c	5.04	5.01	5.01
Distributed polarizabilities:					
H1 H1	00	00		131.56	0.018
	00	10		−90.43	0.025
	10	10		68.10	3.31
	11c	11c		7.36	2.70
H1 H2	00	00		−131.56	−0.018
	00	10		−90.43	0.025
	10	10		59.54	0.01
	11c	11c		−4.85	−0.20
Localized polarizabilities:					
H1 H1	00	00		0.0	0.0
	00	10		0.0	0.0
	10	10		3.41	3.41
	11c	11c		2.50	2.51

further constraint, so that we minimize

$$\Xi_{iv} = \Delta_{iv} - \eta \sum_{a,\, b \neq a} E_{iv}^{ab} + \lambda (d_{iv})^2, \tag{27}$$

where E_{iv}^{ab} is the Coulomb interaction between the contributions of the basis functions of sites a and b to the transition density ρ_{iv}, and is defined as

$$E_{iv}^{ab} = \int\int \frac{\tilde{\rho}_{iv}^{a}(\boldsymbol{r}_1)\tilde{\rho}_{iv}^{b}(\boldsymbol{r}_2)}{r_{12}} \mathrm{d}^3\boldsymbol{r}_1 \mathrm{d}^3\boldsymbol{r}_2. \tag{28}$$

This is effective in removing the non-physical behaviour of the distributed polarizabilities. The parameter λ should properly be treated as a Lagrange multiplier, but it is simpler just to assign a large fixed value to it and to treat the last term of equation (27) as a penalty function. The middle term is also treated as a penalty function. Because ρ_{iv} is a transition density its integral over all space is zero, by orbital orthogonality, and the integral in equation (28) has both positive and negative contributions. The optimum value of η, and even its sign, is not obvious *a priori*, but we have found empirically that η depends only weakly on basis set, and that values in the region of 0.0005 are suitable.

With this modification, the density-fitted form of the FDDS leads to much more sensible values, as shown by the column in table 1 headed $\eta = 0.0005$. However there are still nonlocal polarizabilities, i.e. α_{tu}^{ab} with $a \neq b$, and although they are now very

much smaller, they are still inconvenient – equation (23) requires a double sum over sites.

The non-local polarizabilities can be removed using a method due to Le Sueur and Stone [45]. The moments induced in atom b by a perturbation at atom a are in effect described by a multipole expansion about a. The procedure is in practice somewhat more elaborate in order to ensure that the polarizabilities remain symmetric, $\alpha^{aa}_{tu} = \alpha^{aa}_{ut}$. In the case of H_2, the resulting description is in fact determined by symmetry.

The method has been applied to a number of molecules. Calculations were carried out using the PBE0 functional [15, 51] with asymptotic corrections [16, 17], as described in section 2. The Sadlej basis set [52] was used; although relatively small, it is tuned for polarizabilities, and yields total and distributed polarizabilities that are almost the same as those obtained with the much larger Dunning aug-cc-pVTZ basis, at a much lower computational cost. Results for CO_2, formamide and N-methyl propanamide were reported in [23]. The results are illustrated here for N-methyl propanamide by mapping the induction energy due to a point charge on a surface at twice the van der Waals radius away from the atoms (the vdW×2 surface). For computational convenience the surface was constructed as follows. If the required distance from atom a is R^0_a (twice the van der Waals radius in this case) then the surface is defined by $R_a - R^0_a = 0$, or equivalently $\exp\left[-\xi(R_a - R^0_a)\right] = 1$, where ξ is an arbitrary constant. We define the surface for the whole molecule by $\sum_a \exp\left[-\xi(R_a - R^0_a)\right] = 1$. The effect is as if we shrank an elastic membrane onto the union of vdW×2 atomic surfaces, more or less tightly depending on the value of ξ; the intersections between the vdW surfaces of neighbouring atoms are smoothed out. A value of $\xi = 2$ has been used for the maps shown here. The maps were generated using the ORIENT program, version 4.6 [53].

Figure 1 shows the performance of non-local polarizability models by means of maps of the induction energy ($kJ\,mol^{-1}$) arising from a unit charge on the vdW×2 surface of N-methyl propanamide, both with the non-expanded SAPT(DFT) expression and the rank 4 and rank 2 non-local distributed-multipole approximations. In this and subsequent pictures the heavy-atom backbone of N-methyl propanamide lies in the plane of the picture, with the O atom centre right and the $HNCH_3$ group at the top.

Figure 2 shows maps of the differences between each approximate description and the 'exact' SAPT(DFT) values. It is evident that the rank 1 (dipole–dipole) description is inadequate. The rank 2 description is better, with errors of the order of $2\,kJ\,mol^{-1}$ for a unit charge, or well under $0.5\,kJ\,mol^{-1}$ for a more realistic charge of $0.5e$ or less, since the induction energy is proportional to the square of the charge.

The performance of the local polarizability descriptions is shown in figure 3. As expected, the rank 2 local description is worse than the non-local, but surprisingly the rank 1 local description is somewhat better than the non-local one. Presumably a cancellation of errors is responsible. Nevertheless the description is still inadequate, especially in the region of the O atom, where a good account of the polarizability is needed to account for its behaviour as a hydrogen-bond proton acceptor.

The second method for obtaining a polarizability model [22] starts from a random grid of points in the region between the vdW×2 and vdW×4 surfaces. Using coupled Kohn–Sham perturbation theory, we can compute [23] the response α_{PQ}

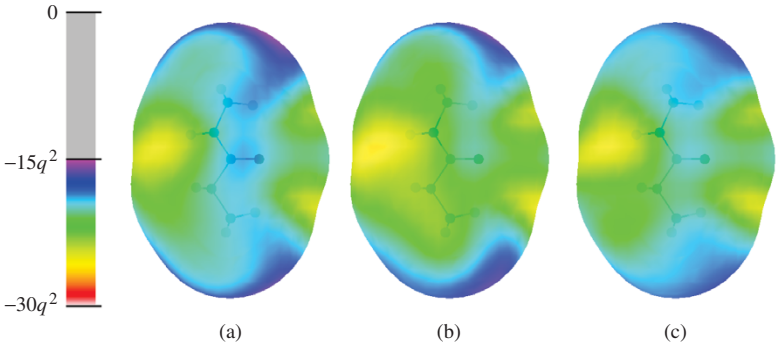

Figure 1. Non-local polarizabilities. Maps of the induction energy (kJ mol^{-1}) arising from a charge q on the vdW × 2 surface of N-methyl propanamide. (a) using the exact coupled Kohn–Sham FDDS, (b) using the rank 4 non-local distributed-multipole approximation and (c) using the rank 2 non-local distributed-multipole approximation.

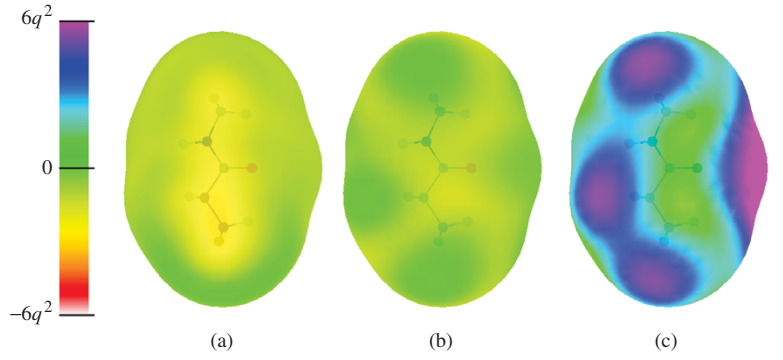

Figure 2. Non-local polarizability errors. Induction energy arising from a charge q on the vdW × 2 surface of N-methyl propanamide. Maps of the difference (kJ mol^{-1}) between various non-local distributed-multipole approximations and the induction energy obtained from the 'exact' coupled Kohn–Sham FDDS, (a) rank 4, (b) rank 2, (c) rank 1.

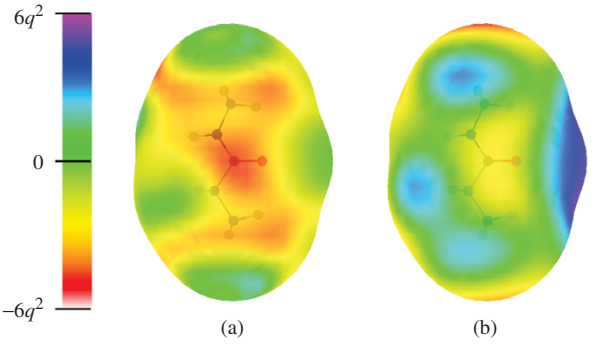

Figure 3. Local polarizability models. Induction energy arising from a charge q on the vdW × 2 surface of N-methyl propanamide. Maps of the difference (kJ mol^{-1}) between various local distributed-multipole approximations and the induction energy obtained from the 'exact' coupled Kohn–Sham FDDS, (a) rank 2, (b) rank 1.

(change in potential) at point P to a point-charge perturbation at Q. For N points we have $1/2\,N(N+1)$ of these responses, and all can be obtained in a single calculation. Then we can postulate a polarizability model of some sort, as simple or as detailed as we wish, and fit the parameters in the model to reproduce the responses as closely as possible in a least-squares sense. If the model comprises polarizabilities α_{tu}^{ab}, then the response at P of the model to a point-charge perturbation at Q is

$$\tilde{\alpha}_{PQ} = \sum_{ab} \sum_{tu} T_{0t}^{Pa} \alpha_{tu}^{ab} T_{u0}^{bQ}, \tag{29}$$

where T_{0t}^{Pa} describes the interaction between a point charge at P and a multipole Q_t at a. Minimizing the sum of squares

$$S = \sum_{PQ} (\tilde{\alpha}_{PQ} - \alpha_{PQ})^2 \tag{30}$$

leads to a set of linear equations for the parameters of the model.

This procedure has a number of attractive features. We can obtain a strictly local model by simply omitting non-local polarizabilities. In the same way, we can avoid charge-flow polarizabilities by leaving them out of the model. The quality of the fit will tell us whether these assumptions are adequate. Furthermore, the procedure is stable and well-conditioned. Unfortunately it does have a disadvantage: the parameters that emerge are not always physically sensible. That is, the atomic polarizabilities are not always positive definite. This in principle means that the induction energy could become positive, which is not physically possible, though it is very unlikely to happen with a physically reasonable external field.

Nevertheless it is better to avoid such non-physical models, and it can be done by combining the fitting procedure with the results of the density-fitting method. Instead of minimizing equation (30), we minimize

$$S = \sum_{PQ} (\tilde{\alpha}_{PQ} - \alpha_{PQ})^2 + \sum_{kk'} g_{kk'} (p_k - p_k^0)(p_{k'} - p_{k'}^0), \tag{31}$$

where the p_k are the parameters of the model, p_k^0 is an 'anchor' or reference value for parameter p_k, and $g_{kk'}$ is a positive definite matrix of coefficients (a diagonal matrix in the simplest case). The 'anchor' values for troublesome atoms can be taken from the localized density-fitting procedure, and the remaining parameters can be fitted without constraints.

Figure 4 shows that the results are very good. Using local dipole–dipole polarizabilities only, the maximum error in the induction energies is only $1.8q^2\,\mathrm{kJ\,mol^{-1}}$, and with a realistic charge q this will be of the order of $0.5\,\mathrm{kJ\,mol^{-1}}$. Applying the constraint to prevent the occurrence of non-physical polarizabilities makes the fit only slightly worse, and does not increase the error in the induction energies at all. This therefore promises to be a very useful approach to the determination of local polarizability models for molecules of significant size. This method has been recently used to calculate distributed polarizabilities up to rank 4 for the 22-atom 3-azabicyclo[3.3.1]nonane-2,4-dione molecule [24].

5.2. *Distributed dispersion*

A method for obtaining atom–atom dispersion coefficients for the case of an atom interacting with a linear molecule has been described by Sanz-Garcia and Wheatley [54], but we need a method that is applicable to more general geometries. The method described above for the induction energy can be extended to dispersion, just by replacing the static polarizabilities with polarizabilities at imaginary frequency. All of the calculations proceed just as easily as in the static case, but they have to be carried out using time-dependent density-functional theory. The polarizabilities are obtained at a set of 10 or so imaginary frequencies, chosen as the abscissae for a Gauss–Legendre quadrature. To obtain the dispersion coefficients in a useful form, it is necessary to recouple the polarizabilities, so that for example the dipole–dipole polarizability is described by a scalar α_{00}, proportional to the mean polarizability $\overline{\alpha}$, and a set of five rank-2 polarizabilities α_{2q} describing any anisotropy. These can then be combined to yield isotropic and anisotropic dispersion coefficients [44, 55, 56].

It is particularly important to exclude non-local polarizabilities, and especially charge-flow polarizabilities, from the dispersion picture. The general form of the asymptotic second-order dispersion energy is

$$E_{\mathrm{disp}}^{(2)} = -\frac{1}{2\pi} \sum_{aba'b'} \sum_{tut'u'} T_{tu}^{ab} T_{t'u'}^{a'b'} \int_0^\infty \alpha_{tt'}^{aa'}(\mathrm{i}v) \alpha_{uu'}^{bb'}(\mathrm{i}v) \mathrm{d}v, \tag{32}$$

where T_{tu}^{ab} describes the electrostatic interaction between multipole t on atom a and multipole u on atom b. The interaction between multipoles of ranks l and l' has a distance dependence $R^{-l-l'-1}$, so a dispersion term involving only charge–charge polarizabilities ($l = l' = 0$ in both T factors) would have distance dependence R^{-2}. Terms in R^{-3}, R^{-4} and R^{-5} would also occur. We know that at long range, the leading term in the dispersion is proportional to R^{-6}, so all of these lower powers of R^{-1} must cancel out, but the numbers are likely to be large and numerical errors would be a serious problem.

Moreover, with any non-local terms in the description, equation (32) involves a quadruple sum over sites, which is likely to be impractical in terms of computer time.

However we have seen that a local polarizability description gives good results for the static polarizability, so we can use it with some confidence for the polarizabilities at imaginary frequency and the dispersion energy. The details of the procedure for determining the atom–atom polarizabilities are otherwise the same as in the static case [23, 24].

The resulting dispersion models have been tested by mapping the dispersion energy between an N-methyl propanamide molecule and a neon atom in contact with it. The reference dispersion energy was calculated using the SAPT(DFT) equivalent of equation (15) on a grid of such points, using the PBE0 functional with asymptotic corrections and the Sadlej basis set as before, and the various approximations were evaluated on the same grid. The dispersion energies in this case are relatively small, since the neon atom is not very polarizable, but a small spherical atom is the most

convenient type of probe for illustrating the behaviour of the approximations that we have tried.

Figure 5 shows the 'exact' dispersion energy and the multipole approximation using two models: one in which atom-atom dispersion terms in R^{-6} and R^{-8} were included, and one using only the R^{-6} terms. The R^{-7} terms contributed very little. Figure 6 shows the differences between these two models and the 'exact'. We see that the R^{-6} terms alone give a rather poor description.

The complete atom–atom description of the dispersion interaction, including all the anisotropic terms on each atom, is very elaborate, involving over 100 independent non-zero parameters, and as always with a description using fitted parameters, we need to enquire whether all the parameters are necessary. Figure 7 shows the effect of dropping all the anisotropic terms, so that each atom is described by just one C_6 and one C_8 coefficient. The errors in such a description are of the order of $0.1\,\mathrm{kJ\,mol^{-1}}$. Moreover the map in figure 7(c) shows that the worst errors arising from the neglect of anisotropy are in the region of the N–H hydrogen, so the model could be improved by including anisotropic terms there without the need to include them for every atom.

6. Second-order exchange energies

The first-order exchange-repulsion energy is the dominant part of the exchange energy, but significant contributions from exchange also arise at second order in perturbation theory [57]. These are the second-order exchange-induction, $E^{(2)}_{\mathrm{exch-ind}}$, and exchange-dispersion, $E^{(2)}_{\mathrm{exch-disp}}$, energies which, as the names suggest, are the exchange counterparts of the induction and dispersion energies. While $E^{(2)}_{\mathrm{exch-disp}}$ is generally quite small, $E^{(2)}_{\mathrm{exch-ind}}$ is comparable in magnitude to $E^{(2)}_{\mathrm{ind}}$ and quenches the induction energy significantly. These energies are computationally inexpensive when computed using SAPT(DFT) and can probably be included together with $E^{(1)}_{\mathrm{exch}}$ when determining the constants in the overlap model for the exchange.

The second-order exchange energies have generally been ignored in calculations on large molecules. While this can be justified for the relatively small $E^{(2)}_{\mathrm{exch-disp}}$ energy, $E^{(2)}_{\mathrm{exch-ind}}$ is generally too large in magnitude to be neglected. That it has been neglected in earlier work without resulting in noticeably large errors is intriguing and is due to a near cancellation of the penetration and truncation errors of the induction models in common use (see section 9) and the neglected second-order exchange-induction energy [24]. However, any attempt at more accurate atom–atom potential development cannot rely on such cancellations, and these exchange components must be included explicitly.

7. Higher-order contributions to the two-body energy

Terms of third and higher order can make important contributions to the interaction energy, particularly for polar molecules, in which case these terms are dominated by higher-order induction and exchange-induction effects [58].

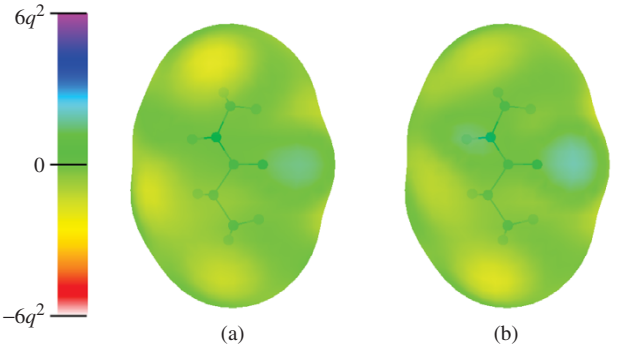

Figure 4. Fitted local polarizabilities. Induction energy arising from a charge q on the vdW × 2 surface of N-methyl propanamide. Maps of the difference (kJ mol^{-1}) between local fitted distributed-multipole models and the induction energy obtained from the 'exact' coupled Kohn–Sham FDDS, (a) rank 1, fitted without constraints, (b) rank 1, fitted with constraints to prevent non-physical polarizabilities.

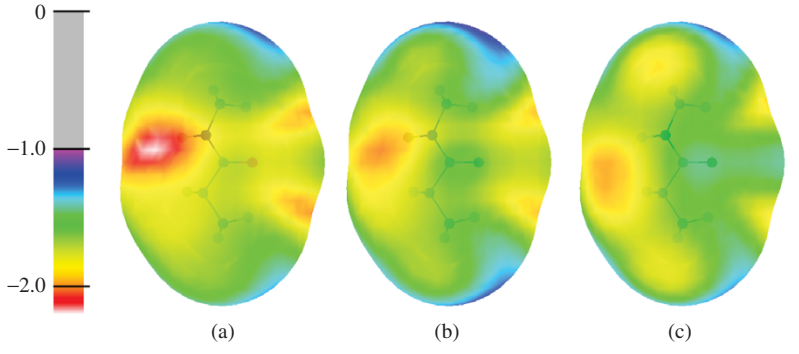

Figure 5. Dispersion energy (kJ mol^{-1}) between a neon atom and N-methyl propanamide, with the atom and molecule in contact as determined by the van der Waals radii. (a) 'exact' CKS results, (b) including R^{-6} and R^{-8} dispersion terms, (c) including R^{-6} dispersion terms only.

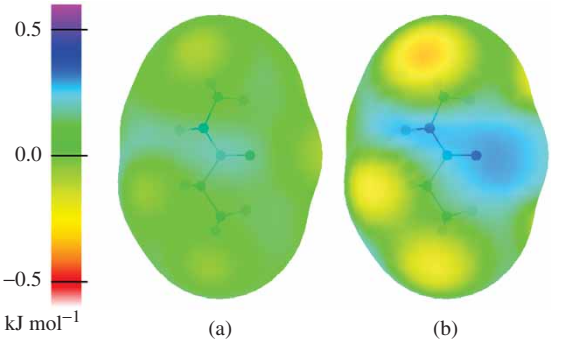

Figure 6. Dispersion energy between a neon atom and N-methyl propanamide, with the atom and molecule in contact as determined by the van der Waals radii. (a) difference between the model including R^{-6} and R^{-8} dispersion terms and the 'exact', (b) difference between the model including R^{-6} dispersion terms only and the 'exact'.

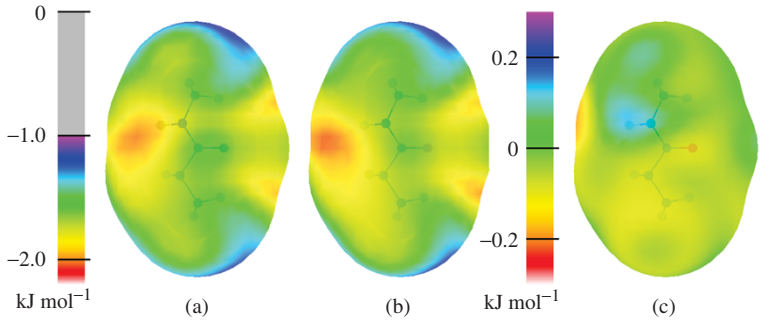

Figure 7. [Colour online] Dispersion energy between a neon atom and N-methyl propanamide, with the atom and molecule in contact as determined by the van der Waals radii, (a) including fully anisotropic R^{-6} and R^{-8} atom–atom dispersion terms, (b) including only the isotropic R^{-6} and R^{-8} atom–atom dispersion terms, (c) anisotropic part of the contribution from the R^{-6} and R^{-8} atom–atom dispersion terms.

The third-order induction and exchange-induction energies [58] cannot at present be computed with response effects included, that is, using coupled perturbation theory, but they can be obtained from uncoupled Kohn–Sham or Hartree–Fock theories. There seems to be evidence [58] that using the uncoupled Hartree–Fock forms of these energies does not account satisfactorily for the higher-order contributions to the interaction energy. An alternative way to calculate these contributions is to use the δ^{HF} term, defined as the difference between the supermolecular Hartree–Fock interaction energy calculated in the dimer basis and the sum of certain low-order SAPT energy terms [57, 59, 60]. δ^{HF} is generally supposed to account for the bulk of higher-order effects for polar systems, but is clumsy to calculate and seems to be inappropriate for non-polar (dispersion bound) systems [58].

The classical polarization model (see [44] for a description) can describe effects which in quantum mechanical perturbation theory would correspond to third and higher order induction terms in the pair interaction energy. Such effects arise when each molecule is polarized by all the others, the induced moment arising from the induced moments as well as the static moments on the other molecules:

$$\Delta Q_t^a = -\sum_{B\neq A}\sum_{b\in B}\sum_{a'\in A}\sum_{t'u}\alpha_{tt'}^{aa'}T_{t'u}^{a'b}(Q_u^b+\Delta Q_u^b). \tag{33}$$

If the ΔQ_u^b term on the r.h.s. is neglected, the resulting energy corresponds to the second-order induction energy. If the induced moments are to be included on the r.h.s., they must be calculated using an iterative procedure, and the resulting energy is the classical induction energy summed to infinite order. The cumulative effect of the iterations is minimal for a dimer, but can be substantial for a cluster and in the condensed phase [24]. Orbital overlap effects, which are neglected in the classical model, also become increasingly important with increasing order of perturbation theory.

Therefore, for the present, there seems to be no convenient way to calculate higher-order contributions to the interaction energy accurately. This is an active field of research [24, 58].

8. Many-body effects

In the condensed phase of water, the two-body interaction energies have been found [61–63] to account for only about 70% of the total interaction energy per molecule. The remaining 30% arises from non-additivity, that is, that part of the interaction energy that cannot be represented by the sum of pair-wise interactions. This nonadditivity is responsible for some of the important structural properties of water, and in particular plays a large role in hydrogen bonding. For example, the tetrahedral structure of water in the liquid state has been attributed to three-body effects [64]. The non-additive effects are expected to be important too for polar molecules other than water, and should be included in atom–atom potentials for organic molecules, which are commonly very polar and often form hydrogen-bonded networks.

The treatment of non-additivity by *ab initio* perturbation theory is difficult, and although there is a version of SAPT that includes the three-body non-additivity (see [57] for a review), the computational demands are so high as to preclude applications to organic molecules. However, one of the conclusions of accurate studies on water clusters [61–63] has been that the bulk of the non-additivity for polar systems can be recovered using the relatively simple classical polarization model (see [44] for a description). While exchange non-additivity is significant for small clusters [61, 62], it is less important in relative terms for large clusters and the condensed phase, because additional coordination shells around any given molecule increase the dispersion and electrostatic energies but not the short-range contributions like exchange non-additivity [63].

There are also many-body terms in the dispersion energy. The leading term is the Axilrod–Teller–Muto triple-dipole dispersion, which for isotropic local distributed polarizabilities takes the form

$$U_{3\mu}^{ABC} = \sum_{a\in A}\sum_{b\in B}\sum_{c\in C} C_9 \frac{(1+3\cos\hat{a}\cos\hat{b}\cos\hat{c})}{R_{ab}^3 R_{bc}^3 R_{ac}^3}, \tag{34}$$

where R_{ab}, etc., are the lengths of the sides and $\hat{a}$, $\hat{b}$ and $\hat{c}$ are the angles of the triangle formed by the three atoms, and

$$C_9 = \frac{3}{\pi}\int_0^\infty \alpha^a(\mathrm{i}u)\alpha^b(\mathrm{i}u)\alpha^c(\mathrm{i}u)\,\mathrm{d}u. \tag{35}$$

A more general expression, allowing for anisotropy and for higher-rank polarizabilities, can be constructed without difficulty. The triple-dipole term is known to contribute significantly, and repulsively, to the lattice energies of the inert gases, but its distance

dependence is R^{-9}, and large molecules have relatively fewer close 3-atom contacts in condensed phases than small ones, so even this term is likely to contribute very much in systems involving molecules of any size.

9. Penetration, truncation errors and damping

The asymptotic expansions described for the electrostatic, induction and dispersion terms cannot be used directly in an atom–atom potential because they are in error in several ways.

- The multipole expansion of the electrostatic interaction treats the charge distribution as if it were concentrated at the expansion origin. The true charge distributions, however, are finite in extent, and the multipole expansion is in error when these extended charge distributions overlap. This error is called the 'penetration error'.
- Similarly, the asymptotic expansions of the induction and dispersion energies also ignore the finite extent of the charge distribution. The penetration error here is the difference between the asymptotic expansion and the non-expanded expression, (14) or (15).
- In addition, 'exchange-dispersion' and 'exchange-induction' terms arise when the molecular wavefunctions overlap.
- Moreover the asymptotic expansion is an infinite series and has to be truncated, usually at quite low order, for practical calculations. This introduces a 'truncation error'.

9.1. *Damping*

The true intermolecular interaction remains finite at all distances, except for R^{-1} divergences arising from nucleus–nucleus repulsion, but the asymptotic series are expansions in inverse powers of the inter-site distance R_{ab}, so they diverge when the sites coincide, always to negative energy in the case of induction and dispersion.

For molecular dynamics at ambient or lower temperatures, the short-range divergence is not usually troublesome, as the kinetic energy is not great enough to overcome the repulsion and reach the divergent regions. In Monte Carlo simulations, however, where a trial step is taken without regard to energy, the system can become trapped in a spurious well. In any case, the incipient divergence in the asymptotic expansion for the dispersion has significant effects at distances near the equilibrium separation. This is clearly demonstrated in the formamide…water example to be discussed below. It is customary to deal with this by using term-by-term 'damping functions', the R^{-n} term being multiplied by a damping function $f_n(R)$ that goes to zero fast enough as $R \to 0$ to cancel out the divergence. The exact choice of damping function remains an outstanding problem, though the Tang–Toennies [65] damping functions, which are incomplete gamma functions, seem to have had the greatest success in the generation of high-accuracy potentials for small dimers. Truncation of the asymptotic series however involves the omission of negative terms, so the magnitude

of the dispersion is underestimated for moderate distances, and the truncated series may need to be enhanced or 'anti-damped' in this region [66].

It is usually assumed, as the notation suggests, that the damping function is independent of orientation, but this assumption is based more on ignorance of how it should behave than on any positive evidence, though Sanz-Garcia and Wheatley found that damping functions in an atom–atom description were more isotropic than those for the intermolecular dispersion energy as a whole [54].

The divergence of the asymptotic expansion for the electrostatic interaction is not troublesome at physically accessible intermolecular separations, and damping is needed only when the potentials are to be used in Monte Carlo simulations.

Induction is troublesome to handle, because the induced moments themselves induce further changes in the moments of neighbouring molecules. For a complete description, it is necessary to iterate the induction process, using the polarized moments at each step to calculate new polarized moments for the next step. The iterative procedure normally converges quite quickly, but it can diverge if the the polarizabilities are large and the separation small. If the molecules are not very polar and not very polarizable, it may be a good enough approximation to calculate the induction energy of each molecule in the field of the unpolarized moments of the others. This non-iterated induction energy doesn't usually seem to need damping, as the non-expanded SAPT(DFT) induction energy is generally larger in magnitude than the asymptotic approximation when terms up to rank 2 are used. However, damping is needed for the iterated induction energy, and can be introduced in the interaction functions T_{tu}^{ab}, but at present it is not clear how it should be described.

9.2. *Penetration*

The multipole expansion of the electrostatic interaction is in error when the molecular charge distributions overlap, even if the multipole expansion still converges. The correction is called the penetration energy, and is negative for small to moderate overlap. In principle the charge density could be separated into atomic contributions, as described for the exchange–repulsion energy, and the difference between the exact electrostatic interaction between two such atomic charge densities and its multipole expansion could then be expanded in a suitable short-range basis. This is not however a satisfactory approach: the true electrostatic interaction between atoms remains finite, apart from the nucleus–nucleus repulsion, so the divergence in the multipole expansion would have to be cancelled by a divergent expansion of the penetration energy.

A more satisfactory treatment would be the use of Wheatley's Gaussian multipoles [31, 67]. In this approach, the charge density is represented by a superposition of Gaussian functions, and the electrostatic interaction can then be represented exactly in analytical form, with no divergences other than the nucleus–nucleus repulsion as $R \to 0$. The disadvantage of this representation is that the expressions for the electrostatic interaction are rather more complicated than for point multipoles – both the initial computation of the Gaussian multipoles and their use in simulations are time-consuming – and they have not been widely adopted, but for some applications the price might be worth paying.

The penetration error can be as large as several kJ mol^{-1} at equilibrium geometries, and cannot be ignored. For the electrostatic energy, it is known to decay roughly exponentially with increasing separation in the region of small overlap, i.e. as $\exp(-\alpha R_{ab})$. This behaviour is similar to that of the repulsion, and because both effects arise from the overlap of electron densities, the exponential coefficient α is similar in magnitude for both. Consequently a common practice is to take the first-order energy from intermolecular perturbation theory, which comprises the electrostatic and exchange–repulsion terms, and subtract the truncated multipole expansion of the electrostatic energy from it to leave the sum of the exchange repulsion and the penetration-truncation corrections. This sum is then fitted to an atom–atom description in the same way as the exchange–repulsion.

9.3. *Penetration effects at second order*

The asymptotic expansions for the second-order energies, i.e. induction and dispersion, are also in error when the molecular wavefunctions overlap. The penetration error here is defined as the difference between the asymptotic expansion and the non-expanded expression (14) or (15). At moderate distances, it is negative for the dispersion energy, but may be positive for the induction energy, so while the asymptotic expansion for the dispersion needs to be damped, the induction expansion may need anti-damping. The object of the damping or anti-damping procedure is to remove the penetration error completely, but the empirical methods in current use cannot be expected to achieve this. Consequently there is a residual penetration error in the damped expansion that may have either sign, and indeed may be positive in some places and negative in others. Moreover there will still be a truncation error.

For these reasons the penetration and truncation corrections at second order are more complicated to model than those at first order. Nevertheless, in model construction much the same approach is taken: the difference between the damped truncated multipole expansion and the basis-saturated non-expanded energy is modelled, together with the second-order exchange-induction and exchange-dispersion energies, using either a Born–Mayer function (equation (9)), or, possibly, the overlap model. In practice it has been customary to include these energies with the first order penetration and exchange energies and to fit them all together.

9.4. *Example: Formamide $\cdots$ water*

In figures 8 and 9, we illustrate the points discussed above by the induction and dispersion energies calculated for the formamide$\cdots$water complex, in two geometries, chosen to emphasise the contacts of particular pairs of atoms and minimize others.

Figure 8 shows the energy difference $\Delta E = E_{\mathrm{ind}}^{\mathrm{asymp}} - E_{\mathrm{ind}}^{(2)}$ between the truncated asymptotic expansion of the induction energy and the non-expanded energy from equation (14). For the curves denoted $L1$, the local polarizabilities used in the expansion are truncated at rank 1 (dipole–dipole), while for $L2$ they are truncated at rank 2 (quadrupole–quadrupole). A positive energy difference means that the asymptotic

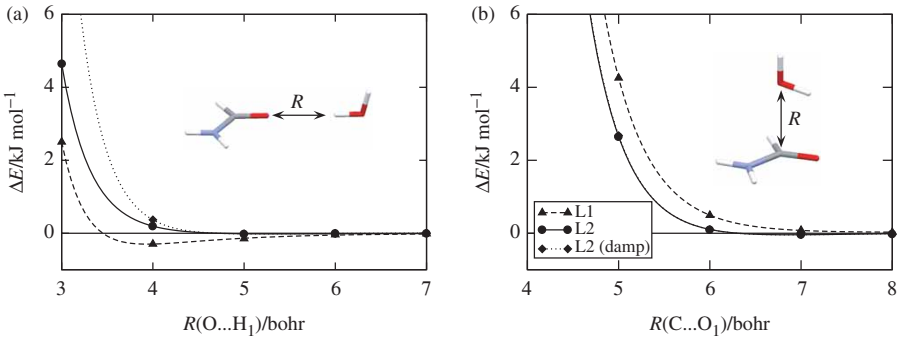

Figure 8. [Colour online] The errors in the asymptotic expansion of induction for the formamide $\cdots$ water dimer in two geometries. In (a) the C and O of formamide and one H and the O from water are collinear, with the second hydrogen in water in the plane perpendicular to the formamide molecule. In (b) the C of formamide and the O of water are in close proximity, with these two atoms and one H of water collinear and the second O–H bond of water in the direction of the C–O bond of formamide. The quantities plotted are the energy differences between each of a number of asymptotic models and the SAPT(DFT) energy. Note that in (b), the damped and undamped L2 models are not visibly distinguishable.

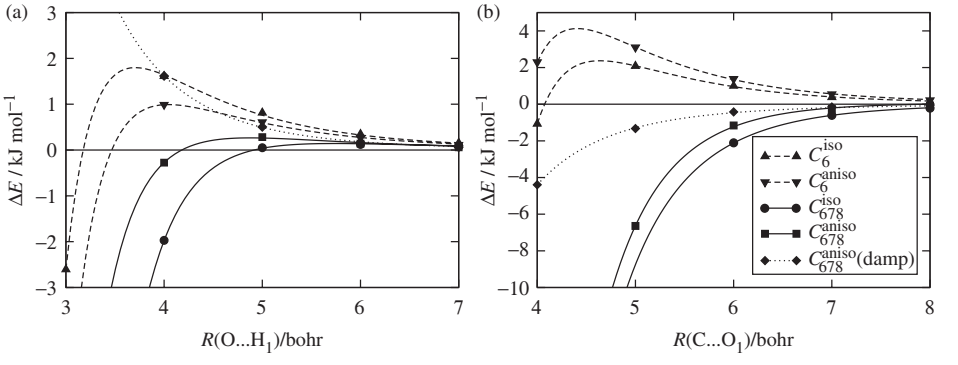

Figure 9. The errors in the asymptotic expansion of dispersion for the formamide $\cdots$ water dimer in the same geometries as in figure 8. The quantities plotted are the energy differences between each of a number of asymptotic models and the SAPT(DFT) energy.

model energy is smaller in magnitude (less negative) than the SAPT(DFT) non-expanded energy. The residual error is quite large, and almost all models seem to need anti-damping to agree with SAPT(DFT). Damping is, however, needed to keep the iterated induction energy finite (see section 7). We do not at present know of a rigorous method for determining the most suitable form of damping; currently we use Tang–Toennies damping functions $f_n(bR)$ for each R^{-n} T function in the induction energy expression, with $b = 1.83$ [34].

For the dispersion, figure 9 shows expansions truncated at R^{-6} atom–atom terms, denoted C_6, and at R^{-8} terms, denoted C_{678}. In both cases the full anisotropic dispersion is shown, and also the result of including only the isotropic atom–atom terms. The damped expansion uses Tang–Toennies damping functions $f_n(bR)$, as above.

In geometry (*a*), all asymptotic models need to be anti-damped at intermediate distances (because of the truncation error) but damped at small distances. The anti-damping needed is less for the C_{678} models, but is rather large for the simpler C_6 models, for which the SAPT(DFT) dispersion energy is underestimated by about $1\,\mathrm{kJ\,mol^{-1}}$ at the minimum. In geometry (*b*), the same holds for the C_6 models, but now the C_{678} models overestimate the dispersion and need to be damped at all distances.

Using the same damping coefficient for both geometries, as here, leads to errors of opposite signs. This could complicate models in which the remaining error (often erroneously assumed to be the penetration error) is assumed to be positive.

The fitting procedure described above (equation (30) or (31)) provides a way to explore the use of damping functions, since the interaction functions T^{ab}_{tu} that appear in (29) may include a damping function. If this is done, the fitted polarizabilities and dispersion coefficients that result are the values that are most suitable for use with those damped interaction functions. It would be necessary to choose the points to be used in the fitting procedure closer to the molecule than 2–4 times the van der Waals radius, in order to sample the region where the damping functions become effective.

10. Other considerations

10.1. *Basis sets*

The basis set requirements for accurate calculations of molecular properties and intermolecular interaction energies tend to be quite stringent. Firstly, intermolecular energies are strongly dependent on the asymptotic regions of the molecular wave functions, and diffuse basis functions are required to describe these parts of the wave function accurately. Modern *augmented* basis sets of triple-zeta quality generally satisfy this requirement.

Secondly, the dispersion energy is very slowly convergent with respect to the rank of the angular functions included in the basis [68]. This is probably because the penetration contribution of the intermolecular correlation responsible for the dispersion arises from the region between the interacting molecules, and is consequently hard to describe with basis functions centred on the atomic sites. It has been observed that adding a small set of basis functions in the bonding region (the so-called 'mid-bond' functions) improves the convergence of the dispersion significantly [68]. The effect of these mid-bond functions is not at all small; they can account for as much as 20% of the dispersion energy at the equilibrium distance, and more at shorter separations. If the basis set used for the calculations reported in figure 9 was augmented with such mid-bond functions, the anti-damping needed for the dispersion would be even greater. This point is generally missed in calculations on large molecules but needs to be adequately addressed.

Further complications are introduced by the extreme sensitivity of both second-order induction and exchange-induction energies to the presence of basis functions located on the atomic sites of the interacting partner. These basis functions, sometimes referred to as 'far-bond' functions [68], lead to short-range induction and exchange-induction

energies that can be orders of magnitude larger than their counterparts calculated in monomer basis sets. One consequence of this sensitivity is that the basis-saturated induction energy is generally much larger in magnitude than the asymptotic expansion would suggest, so that the asymptotic expansions need to be enhanced rather than damped even more than has been shown in figure 8. There is some debate as to whether this unusual behaviour is a charge transfer effect [69] or a manifestation of the divergence of the induction series due to the Coulomb singularities in the intermolecular operator [70, 71]. The development of a regularized symmetry-adapted perturbation theory, that is, a perturbation theory without the Coulomb singularities, is an active field of research [71]. While there is an indication that the pathological terms in the induction can be removed by regularization, there still remain important issues that need to resolved. Furthermore, a regularized version of SAPT(DFT) is yet to be developed. For the present, we believe that the induction energy should be calculated either using a monomer basis augmented with the 'far-bond' functions or in the dimer basis set [24].

10.2. *Molecular geometry*

Computational limitations usually demand that *ab initio* intermolecular potentials are constructed with the molecules kept rigid, generally at the gas phase equilibrium geometry. A better choice has been shown [72] to be the vibrationally averaged molecular geometry, but that is often hard to obtain, as the accurate spectroscopic data needed are not often available. While vibrationally-averaged geometries have been used with good success for small molecules in the gas phase (see [57] for a review), this too may be completely inadequate in the condensed phase where molecules undergo considerable distortion.

For the case of molecular crystals, the molecular distortion in the condensed phase is generally unique and can, at least in principle, be determined by theoretical or experimental methods. Knowledge of the condensed phase and gas phase molecular geometries can then be used to construct the PES using equation (2) – that is, by calculating the surface for the distorted geometries, $V^*_{ABC\ldots}$, and adding on the energy penalties for molecular distortion.

However, the condensed phase geometry may not be unique (as is the case for liquids) or even if unique, may be impossible to predict *a priori* (see [73] for a review). In such cases, the PES involving intermolecular and intramolecular degrees of freedom must be considered. This is a formidable task, and the naive construction of such a surface for even the smallest organic molecule is almost impossible. One possible way to construct such a PES is to include the intramolecular degrees of freedom via a truncated Taylor expansion [74]. This method is computationally efficient and has been demonstrated to result in potentials of spectroscopic accuracy, but as yet it has been applied to small systems only. Another possibility is to use the so-called atom-following approach, i.e., to allow the sites in a site–site potential to move and carry the unchanged site properties with them. This method has the advantage of involving no additional computational expense, but while it is capable of predicting the trends correctly, it is inadequate for the generation of accurate potential energy surfaces [75].

The atom-following approach is based on two assumptions: (1) that the site properties are in some sense physical as opposed to being just mathematical entities, and (2) they don't change very much with molecular distortion. The latter issue has been addressed [75] by introducing an explicit molecular geometry dependence in the asymptotic coefficients for the dispersion and induction energies. This has been found to work better than the naive atom-following approach. Further improvements are probably possible if the site properties are obtained in a physical manner, perhaps using the distribution techniques described above.

Finally, there are cases where the changes in molecular structure in the condensed phase is so large as to cast doubt on the possibility of using perturbation theory at all. Zwitterionic systems like glycine fall into this category. The rigorous treatment of such systems remains an open question.

11. Conclusions

The field of intermolecular interactions has seen significant developments in the last few years. The size of system that can be studied has increased to the point where molecules of biological interest can be studied to good accuracy. Theoretical methods like SAPT(DFT) now allow us to calculate accurate interaction energies between pairs of benzene molecules, or other molecules of similar size, on a routine basis. Even molecules such as 3-azabicyclo[3.3.1]nonane-2,4-dione dimer [24] (22 atoms per molecule) can be handled, though this remains a time-consuming calculation. New distribution schemes for both multipole moments and frequency-dependent polarizabilities provide us with the necessary tools for the development of atom–atom potentials. However, these modern accurate *ab initio* calculations of intermolecular interaction energies by perturbation theory have also raised new questions to which satisfactory answers are not yet available. These questions concern the accurate calculation of the interaction energy at short range, where overlap effects are important. This review has attempted to describe all of these topics in some detail, and to show how a new generation of atom–atom potentials can be developed for use in simulations, using the separation of the interaction energy into physically meaningful components that perturbation theory can provide.

For systems of a few atoms, *ab initio* electronic structure theory has already achieved an accuracy high enough to be comparable to the accuracy of experiments. We hope that we will soon be in a position to provide a similar accuracy and predictive power for systems comprising small organic molecules.

12. Programs

Many of the theoretical methods described in this review are implemented in programs available for download. Some of these, together with their main uses in the present work, are:

- SAPT2002 [76]: SAPT(KS) energy calculations.
- SITUS 4.5 [77]: Molecular properties in total and distributed form and SAPT(DFT) dispersion and induction energies.

- ORIENT 4.6 [53]: Localization of the distributed polarizabilities and visualization of the energy maps.
- DALTON 2.0 [78]: DFT and CKS calculations. A patch [76] is needed to enable DALTON 2.0 to work with SAPT2002 and SITUS 4.5.

References

[1] B. Jeziorski, R. Moszynski, and K. Szalewicz. Chem. Rev. **94**, 1887 (1994).
[2] E. M. Mas, K. Szalewicz, R. Bukowski, and B. Jeziorski. J. Chem. Phys. **107**, 4207 (1997).
[3] R. Bukowski, J. Sadlej, B. Jeziorski, P. Jankowski, K. Szalewicz, S.A. Kucharski, H. L. Williams, and B. M. Rice. J. Chem. Phys. **110**, 3785 (1999).
[4] A. J. Misquitta and K. Szalewicz. Chem. Phys. Lett. **357**, 301 (2002).
[5] A. J. Misquitta, B. Jeziorski, and K. Szalewicz. Phys. Rev. Lett. **91**, 33201 (2003).
[6] A. Hesselmann and G. Jansen. Chem. Phys. Lett. **357**, 464 (2002).
[7] A. Hesselmann and G. Jansen. Chem. Phys. Lett. **362**, 319 (2002).
[8] A. Hesselmann and G. Jansen. Chem. Phys. Lett. **367**, 778 (2003).
[9] R. Podeszwa, R. Bukowski, and K. Szalewicz. J. Chem. Theory Comput. **2**, 400 (2006).
[10] R. Podeszwa, R. Bukowski, and K. Szalewicz. J. Phys. Chem. A **110**, 10345 (2006).
[11] H. L. Williams and C. F. Chabalowski. J. Phys. Chem. A **105**, 646 (2001).
[12] A. J. Misquitta and K. Szalewicz. J. Chem. Phys. **122**, 214109 (2005).
[13] R. Moszynski, B. Jeziorski, S. Rybak, K. Szalewicz, and H. L. Williams. J. Chem. Phys. **100**, 5080 (1994).
[14] A. J. Misquitta, R. Podeszwa, B. Jeziorski, and K. Szalewicz. J. Chem. Phys. **123**, 214103 (2005).
[15] C. Adamo and V. Barone. J. Chem. Phys. **110**, 6158 (1999).
[16] D. J. Tozer and N. C. Handy. J. Chem. Phys. **109**, 10180 (1998).
[17] D. J. Tozer. J. Chem. Phys. **112**, 3507 (2000).
[18] A. Hesselmann, G. Jansen, and M. Schutz. J. Chem. Phys. **122**, 014103 (2005).
[19] A. J. Stone. Chem. Phys. Lett. **83**, 233 (1981).
[20] A. J. Stone and M. Alderton. Molec. Phys. **56**, 1047 (1985).
[21] A. J. Stone. J. Chem. Theory Comput. **1**, 1128 (2005).
[22] G. J. Williams and A. J. Stone. J. Chem. Phys. **119**, 4620 (2003).
[23] A. J. Misquitta and A. J. Stone. J. Chem. Phys. **124**, 024111 (2006).
[24] A. J. Misquitta, A. J. Stone, and S. L. Price. J. Chem. Phys. (2007). in preparation.
[25] R. Rein. Adv. Quantum Chem. **7**, 335 (1973).
[26] A. T. Amos and R. J. Crispin. Molec. Phys. **31**, 159 (1976).
[27] W. A. Sokalski and R. A. Poirier. Chem. Phys. Lett. **98**, 86 (1983).
[28] F. Vigné-Maeder and P. Claverie. J. Chem. Phys. **88**, 4934 (1988).
[29] P. L. A. Popelier and M. Rafat. Chem. Phys. Lett. **376**, 148 (2003).
[30] R. Bader. *Atoms in Molecules* (Clarendon Press, Oxford, 1990).
[31] R. J. Wheatley and J. B. O. Mitchell. J. Comput. Chem. **15**, 1187 (1994).
[32] S. L. Price and A. J. Stone. Molec. Phys. **47**, 1457 (1982).
[33] A. J. Stone and S. L. Price. J. Phys. Chem. **92**, 3325 (1988).
[34] A. J. Misquitta and A. J. Stone. J. Chem. Phys. (2007). in preparation.
[35] I. Nobeli and S. L. Price. J. Phys. Chem. A **103**, 6448 (1999).
[36] H. C. Longuet-Higgins. Disc. Faraday Soc. **40**, 7 (1965).
[37] M. E. Casida. In *Recent Advances in Density-Functional Theory*, edited by D. P. Chong, (World Scientific, 1995).
[38] M. Petersilka, U. J. Gossmann, and E. K. U. Gross. Phys. Rev. Lett. **76**, 1212 (1996).
[39] S. M. Colwell, N. C. Handy, and A. M. Lee. J. Chem. Phys. **53**, 1316 (1996).
[40] G. Onida, L. Reinig, and A. Rubio. Rev. Mod. Phys. **74**, 601 (2002).
[41] B. I. Dunlap, J. W. D. Connolly, and J. R. Sabin. J. Chem. Phys. **71**, 4993 (1979).
[42] B. I. Dunlap. Phys. Chem. Chem. Phys. **2**, 2113–2116 (2000).
[43] R. Bukowski, R. Podeszwa, and K. Szalewicz. Chem. Phys. Lett. **414**, 111 (2005).
[44] A. J. Stone. *The Theory of Intermolecular Forces*, International Series of Monographs in Chemistry (Clarendon Press, Oxford, 1996).
[45] C. R. Le Sueur and A. J. Stone. Molec. Phys. **83**, 293 (1994).
[46] J. G. Ángyán, G. Jansen, M. Loos, C. Hättig, and B. A. Heß. Chem. Phys. Lett. **219**, 267 (1994).
[47] F. Dehez, C. Chipot, C. Millot, and J. Ángyán. Chem. Phys. Lett. **338**, 180 (2001).

[48] C. R. Le Sueur and A. J. Stone. Molec. Phys. **78**, 1267 (1993).
[49] L. Gagliardi, R. Lindh, and G. Karlström. J. Chem. Phys. **121**, 4494 (2004).
[50] A. J. Stone. Molec. Phys. **56**, 1065 (1985).
[51] J. Perdew, K. Burke, and M. Ernzerhof. Phys. Rev. Lett. **77**, 3865 (1996). also see erratum, Phys. Rev. Lett. 78, 1396 (1996).
[52] A. J. Sadlej. Theor. Chim. Acta **79**, 123 (1991).
[53] A. J. Stone, A. Dullweber, O. Engkvist, E. Fraschini, M. P. Hodges, A. W. Meredith, D. R. Nutt, P. L. A. Popelier, and D. J. Wales. Orient: a program for studying interactions between molecules, version 4.6. University of Cambridge (2006). Enquiries to A. J. Stone, ajs1@cam.ac.uk.
[54] A. Sanz-Garcia and R. J. Wheatley. Phys. Chem. Chem. Phys **5**, 801 (2003).
[55] A. J. Stone and R. J. A. Tough. Chem. Phys. Lett. **110**, 123 (1984).
[56] G. J. Williams. *Molecular Distributed Polarizabilities*, PhD thesis, University of Cambridge (2004).
[57] B. Jeziorski and K. Szalewicz. In *Handbook of Molecular Physics and Quantum Chemistry*, edited by S. Wilson, (Wiley, 2002), vol. 3, chap. 8, p. 37.
[58] K. Patkowski, K. Szalewicz, and B. Jeziorski. J. Chem. Phys. **125**, 154107 (2006).
[59] M. Jeziorska, B. Jeziorski, and J. Čižek. Int. J. Quantum Chem. **32**, 149 (1987).
[60] R. Moszynski, T. G. A. Heijmen, and B. Jeziorski. Molecular Phys. **88**, 741 (1996).
[61] M. P. Hodges, A. J. Stone, and S. S. Xantheas. J. Phys. Chem. A **101**, 9163 (1997).
[62] A. Milet, R. Moszynski, P. E. S. Wormer, and A. van der Avoird. J. Phys. Chem. A **103**, 6811 (1999).
[63] E. M. Mas, R. Bukowski, and K. Szalewicz. J. Chem. Phys. **118**, 4404 (2003).
[64] R. Bukowski, K. Szalewicz, G. Groenenboom, and A. van der Avoird. J. Chem. Phys. **125**, 044301 (2006).
[65] K. T. Tang and J. P. Toennies. J. Chem. Phys. **80**, 3726 (1984).
[66] M. P. Hodges and A. J. Stone. Molec. Phys. **98**, 275 (2000).
[67] R. J. Wheatley. Molec. Phys. **79**, 597 (1993).
[68] H. L. Williams, E. M. Mas, K. Szalewicz, and B. Jeziorski. J. Chem. Phys. **103**, 7374 (1995).
[69] A. J. Stone. Chem. Phys. Lett. **211**, 101 (1993).
[70] K. Patkowski, B. Jeziorski, and K. Szalewicz. J. Mol. Struct. (TheoChem) **547**, 293 (2001).
[71] K. Patkowski, B. Jeziorski, and K. Szalewicz. J. Chem. Phys. **120**, 6849 (2004).
[72] M. Jeziorska, P. Jankowski, K. Szalewicz, and B. Jeziorski. J. Chem. Phys. **113**, 2957 (2000).
[73] S. L. Price and L. S. Price. In *Structure and Bonding*, (Springer, Berlin/Heidelberg, 2005), vol. 115 (Intermolecular Forces and Clusters, vol. 1), p. 81.
[74] P. Jankowski. J. Chem. Phys. **121**, 1655–1662 (2004).
[75] G. Murdachaew and K. Szalewicz. Faraday Disc. **118**, 121 (2001).
[76] R. Bukowski, W. Cencek, P. Jankowski, B. Jeziorski, M. Jeziorska, S. Kucharski, A. J. Misquitta, R. Moszynski, K. Patkowski, S. Rybak, K. Szalewicz, H. Williams, and P. Wormer. SAPT2002: an ab initio program for many-body symmetry-adapted perturbation theory calculations of intermolecular interaction energies. University of Delaware and University of Warsaw (2002).
[77] A. J. Misquitta and A. J. Stone. SITUS: a program for studying intermolecular interactions and for the calculation of molecular properties in distributed form. University of Cambridge (2006). Enquiries to A. J. Misquitta, am592@cam.ac.uk.
[78] DALTON, a molecular electronic structure program, release 2.0 (2005). See http://www.kjemi.uio.no/software/dalton/dalton.html.